

## Mitigation Of Fretting Fatigue Damage In Blade And Disk Pressure Faces With Low Plasticity Burnishing

**Paul S. Prevéy**

Lambda Technologies  
3929 Virginia Avenue, Cincinnati, Ohio 45227  
United States  
Phone: 513.561.0883, Fax: 513.561.0886  
E-mail: [pprevvey@lambdatechs.com](mailto:pprevvey@lambdatechs.com)

**N. Jayaraman**

Lambda Technologies  
3929 Virginia Avenue, Cincinnati, Ohio 45227  
United States  
Phone: 513.561.0883, Fax: 513.561.0886  
E-mail: [njayaraman@lambdatechs.com](mailto:njayaraman@lambdatechs.com)

**Ravi A. Ravindranath, Propulsion & Power**  
NAVAIR

22195 Elmer Rd., Patuxent River, Maryland  
20670-1534, United States  
Phone: 301.757.0472, Fax: 301.757.0562  
E-mail: [ravi.ravindranath@navy.mil](mailto:ravi.ravindranath@navy.mil)

**Dr. Michael Shepard**

WPAFB AFRL/MLLMN  
2230 10<sup>th</sup> Street, WPAFB, Ohio 45433-7817  
Phone: 937.255.1384, Fax: 937.656.4840  
United States  
E-mail: [michael.shepard@wpafb.af.mil](mailto:michael.shepard@wpafb.af.mil)

### ABSTRACT

Low Plasticity Burnishing (LPB) is now established as a surface enhancement technology capable of introducing through-thickness compressive residual stresses in the edges of gas turbine engine blades and vanes to mitigate foreign object damage (FOD). The "Fatigue Design Diagram" (FDD) method has been described and demonstrated to determine the depth and magnitude of compression required to achieve the optimum high cycle fatigue (HCF) strength, and to mitigate a given depth of damage characterized by the fatigue stress concentration factor,  $k_f$ . LPB surface treatment technology and the FDD method have been combined to successfully mitigate a wide variety of surface damage ranging from FOD to corrosion pits in titanium and steel gas turbine engine compressor and fan components. LPB mitigation of fretting induced damage in Ti-6AL-4V in laboratory samples has now been extended to fan and compressor components.

LPB tooling technology recently developed to allow the processing of the pressure faces of fan and compressor blade dovetails and mating disk slots is described. Fretting induced micro-cracks that form at the pressure face edge of bedding on both the blade dovetail and the dovetail disk slots in Ti-6-4 compressor components can now be arrested by the introduction of deep stable compression in conventional CNC machine tools during manufacture or overhaul. The compressive residual stress field design method employing the FDD approach developed at Lambda Technologies is described in application to mitigate fretting damage. The depth and magnitude of compression and the fatigue and damage tolerance achieved are presented. It was found that micro-cracks as deep as 0.030 in., (0.75 mm) large enough to be readily detected by current NDI technology, can be fully arrested by LPB. The depth of compression achieved could

allow NDI screening followed by LPB processing of critical components to reliably restore fatigue performance and extend component life.

### INTRODUCTION

Fretting initiated fatigue has long been recognized as a major cause of blade dovetail and disk slot failures in aircraft turbine engines.<sup>1,2,3</sup> Extensive research in the areas of contact mechanics,<sup>4,5</sup> crack initiation mechanisms<sup>6,7</sup> and the failure process<sup>8,9</sup> have led to a good understanding of the factors involved in the initiation and propagation of fretting damage. Because fretting fatigue damage occurs under complex mechanical loading and load-interactions between the two contacting surfaces, several factors affect the fatigue performance. These include contact geometry, interfacial friction, and the forces (sliding and normal) acting on the contact face in addition to the usual fatigue conditions of stress ratio ( $R=S_{min}/S_{max}$ ), frequency, and loading mode (axial, bending, etc.). Fretting damage arises from partial slip at the edge of the contact area or edge-of-bedding (EOB). Repeated sliding in the partial slip region surrounding the stick regime frequently results in oxidation of the fretted surface<sup>10</sup> and an accumulation of powdered oxide wear debris. Fatigue cracking initiates from microplasticity in the partial slip region producing microcracking in the form of shallow mode II shear cracks at the edge of contact.<sup>11</sup> The final failure of the part ensues through mode I fatigue crack propagation from these fretting-induced microcracks.

Lubricants and anti-fretting coatings reduce the coefficient of friction and mitigate fretting fatigue damage by reducing the shear stress in the slip region. Fretting in turbine engine dovetail blade/disk contact surfaces is commonly reduced with Cu-Ni-In coatings and MoS<sub>2</sub> dry surface lubricant.<sup>12</sup> Coatings

are applied by a variety of methods including thermal spray, plasma spray, CVD (chemical vapor deposition), PVD (physical vapor deposition), and IBED (ion beam enhanced deposition). The major disadvantage of anti-fretting coatings is that the component performance depends upon the integrity of the coating/lubricant system during service. Continuous rubbing at the contact surface during operation tends to remove the lubricant and wear away the coating eventually exposing the base metal to fretting damage.

A new approach to mitigate fretting fatigue damage has emerged through the use of surface treatment processes that impose deep compressive residual stresses.<sup>13,14,15,16,17,18</sup> Several methods, including shot peening, cavitation peening, laser shock peening (LSP), and low plasticity burnishing (LPB) are available to introduce compression. This approach does not eliminate fretting damage on the contact surface because a compressive mean stress does not affect the cyclic shear stress that creates the microcracks. Rather, the residual compressive mean stress ahead of the microcracks arrests the propagation of the fretting induced shear cracks eliminating fatigue cracking and failure. The effectiveness of the compressive residual stress technologies in mitigating fretting fatigue failure depends upon the depth and magnitude of compression, and the stability of the compressive residual stresses during further processing of components and in service. Shot peening and cavitation peening produce relatively shallow compression, while LPB and LSP impart relatively deep compressive residual stresses, well beyond the depth of fretting induced microcracks.

The potential for relaxation of the compressive residual stresses in components exposed to mechanical overload or elevated temperature depends significantly upon the cold work introduced during surface treatment processes. Typically, shot peening leads to excessive cold work (often > 80%), while LPB and LSP result in very low cold work (<5%) insuring that the beneficial compression is retained during extended service. Attempts are also being made to develop duplex processes, by applying the coatings/lubricant systems after imparting the compressive residual stress<sup>19</sup> through surface treatments. Since most of the coating processes lead to heating the surfaces or are done at elevated temperatures, the stability of compressive residual stresses will be affected by the amount of cold work.

The differences in the nature of the subsurface compressive residual stress distributions imparted by different methods lead to varying degrees of improvement in fretting fatigue resistance. Shallow compression from conventional shot peening significantly improves fretting fatigue performance, but does not fully mitigate fretting induced fatigue failure. When used in conjunction with coatings, the effectiveness of shot peening to improve fretting fatigue resistance is significantly reduced.<sup>20</sup> These deficiencies are attributed to the relatively shallow depth of compression, typically 0.005 in. (0.125 mm) deep, and the heavy cold work associated with the shot peened surface. Several independent studies have now shown that the deeper compressive residual stresses from LPB with low cold work have resulted in complete mitigation of fretting fatigue damage.<sup>14,17,18</sup>

This paper describes recent developments in: (a) the fatigue design methodologies to determine the magnitude and distribution of compression needed to mitigate fretting fatigue, (b) LPB tooling developed to process the complex geometries of turbine compressor blade dovetails and the disk slot contact regions, and (c) the importance of taking a comprehensive design approach by including residual stress measurements to verify and validate the design process.

## MATERIALS AND METHODS

### COMPONENTS AND CHARACTERIZATION OF FRETTING DAMAGE IN UNTREATED COMPONENTS

Photographs of a Ti-6Al-4V compressor blade and disk are shown in Figures 1 and 2, as close-up views of the fretting affected edge-of-contact regions. Figure 3(a) shows a typical network of parallel microcracks found in the dovetail edge-of-bedding. A micrograph of the cross-section, Figure 3(b), shows the depth of the microcrack (arrows) is less than 0.003 in (0.075 mm).

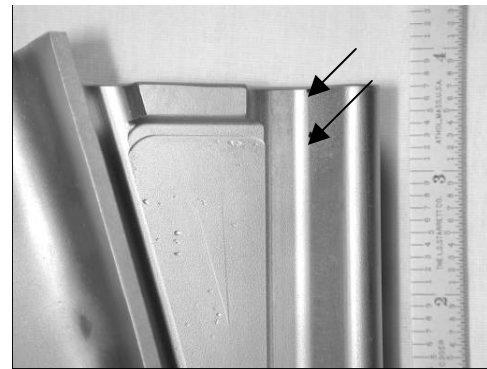
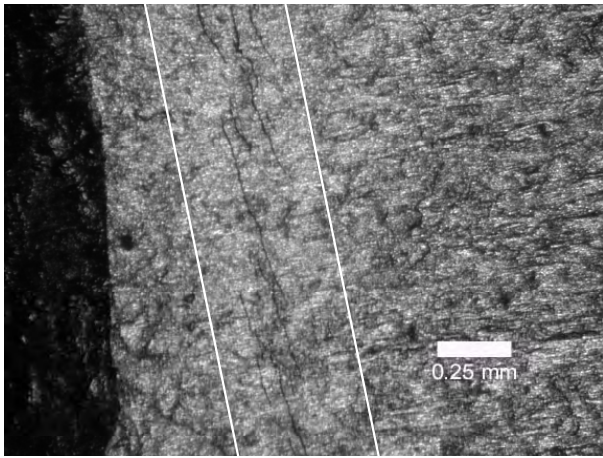


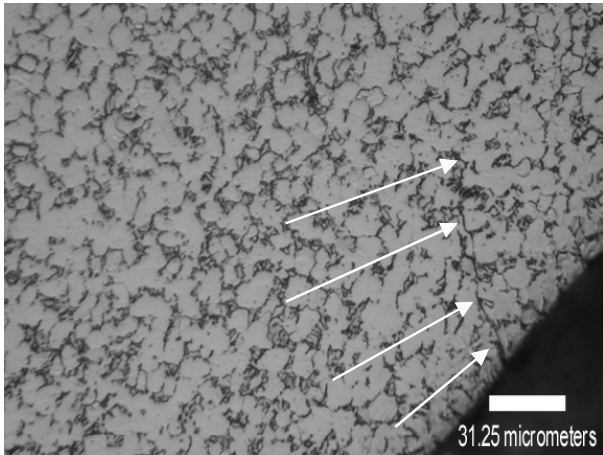
**FIGURE 1** - A close-up view of the dovetail edge-of-bedding region prone to microcracking (dark arrows) due to fretting.



**FIGURE 2** - A close-up view of the dovetail disk post slots.



(a)



(b)

**FIGURE 3** - (a) Optical photo of typical network of parallel microcracks found in the dovetail edge-of-bedding. (b) Optical micrograph of the cross-section showing the depth of the microcrack (arrows). As seen here, the fine microcrack is less than 0.003 in. (0.08 mm) deep from the surface.

**FATIGUE DESIGN METHOD**

The implementation of sophisticated surface enhancement technologies like LPB to induce deep, controlled compressive residual stresses require the use of advanced predictive and design tools, so that the LPB treatment parameters can be optimized for a given application and component. In this context, three major predictive and design analyses tools are being used, viz., linear elastic fracture mechanics (LEFM) based fatigue crack growth codes like AFGROW,<sup>21</sup> finite element (FE) codes like ALGOR and ANSYS, and Lambda’s FDD<sup>22</sup> to predict fatigue performance in the presence of compressive RS in components. The optimal compressive residual stress distribution is determined iteratively by introducing the compressive residual stress from FDD into the FE model and determining both the magnitude and locations of compensatory tension and part-distortion.

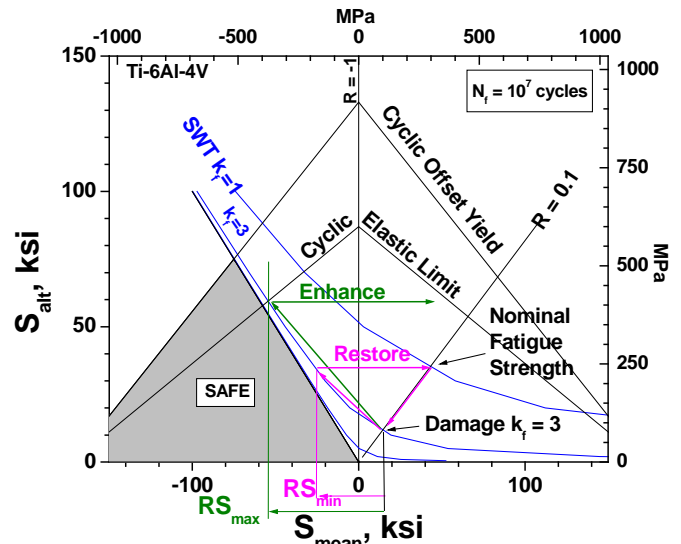


**FIGURE 4** – Fatigue Design Diagram For Ti-6Al-4V to demonstrate the method of determination of minimum and maximum residual compression to restore or enhance fatigue performance.

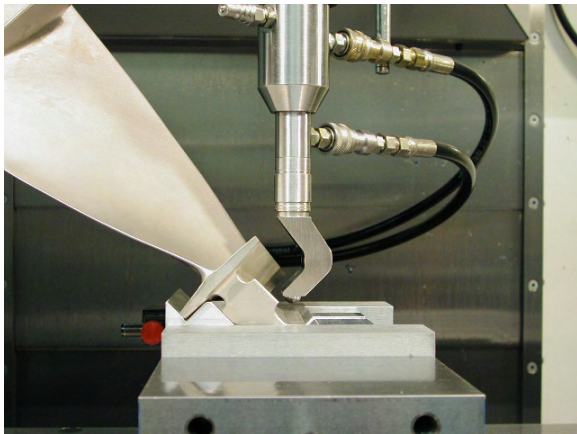
The FDD is a novel adaptation of the traditional Haigh diagram to estimate the compressive residual stress magnitude and distribution to achieve optimal fatigue performance. This method is demonstrated for Ti-6Al-4V in Figure 4, which is a plot of the mean stress ( $S_{mean}$ ) extended into the compressive quadrant vs. alternating stress ( $S_{alt}$ ). The traditional fatigue design approach using the Goodman line in the tensile mean stress quadrant does not lend itself to the analysis of fatigue performance under compressive mean stresses. The Smith-Watson-Topper (SWT) model<sup>23</sup> is valid for mean stresses in both tension and compression. By combining the fatigue stress concentration factor,  $k_f$  (ratio of fatigue strength for a given life for the smooth condition over the damaged condition) with the SWT model, a series of curves can be drawn in place of the Goodman lines for various  $k_f$  values representing levels of damage. Figure 4 shows the construction of the SWT lines for  $k_f = 1, 3$  and  $10$ .

As seen in Figure 4, the limiting cases of  $k_f = \infty$ , and  $R = -\infty$  define a region where the stress state will never go into tension, and hence Mode I crack growth is not possible. This region is indicated as the “SAFE” region. For damage producing a known fatigue debit, say  $k_f = 2.8$  for fretting of Ti-6Al-4V, the FDD allows the determination of the minimum residual compression ( $RS_{min}$ ) needed to restore the fatigue performance and the amount of compression ( $RS_{max}$ ) that will provide the maximum possible fatigue performance. The FDD has been validated in a number of material systems.<sup>24</sup>

**LPB PROCESS**

LPB is a surface treatment that develops a deep layer of high compression on surfaces to mitigate fretting, corrosion pitting, or FOD. Through-thickness compression can be achieved in thin sections, such as blade edges, providing dramatically improved damage tolerance.<sup>25</sup> LPB tools are designed to allow access to the fatigue critical areas of the

component. Examples of LPB tools designed to treat the dovetail region of a compressor blade and the dovetail post contact surface in a compressor disk are shown in Figures 5(a) and 5(b), respectively.



(a)



(b)

**FIGURE 5** – (a) LPB processing of the surface of a Ti-6Al-4V compressor blade dovetail contact region using a specially designed LPB tool. (b) LPB processing of a Ti-6Al-4V compressor disk dovetail post contact region using a specially designed LPB tool.

The LPB process itself has been described in detail previously.<sup>26</sup> Unlike other burnishing or "deep rolling" methods, a single pass of a smooth free rolling spherical ball tool, as shown in Figure 6, is used under a normal force just sufficient to deform the surface of the material, creating a compressive layer of residual stress with controlled plastic deformation. The LPB tool path and position are controlled in a CNC machine tool or robotically in a machine shop environment. Any surface topography that can be followed with a multi-axis CNC tool and allows tool access can be LPB processed. LPB can produce high compression to a depth exceeding 1 mm in thick sections and entirely through thin sections such as structural sheet or the edges of titanium alloy fan blades in 4-axis or 5-axis CNC processing.<sup>27,28</sup> As the ball rolls over the component, the pressure from the ball causes plastic deformation to occur in the surface of the material under the ball. Since the bulk of the material constrains the deformed area, the deformed zone is left in compression after the ball passes. No material is removed during the process.

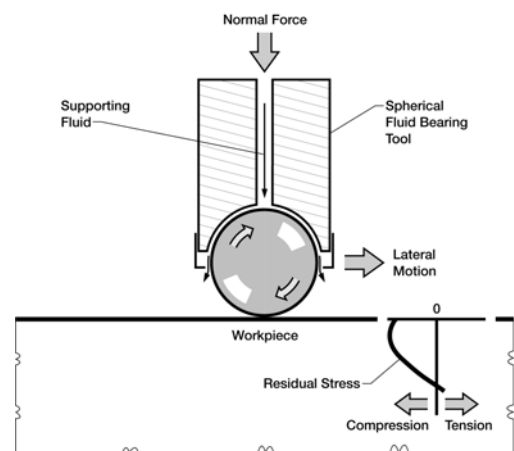


**FIGURE 6** - LPB Schematic

The surface is permanently displaced inward by only a few ten-thousandths of an inch (0.0001-0.0006 in., (2-15  $\mu\text{m}$ )). LPB smoothes surface asperities leaving an improved surface finish that can be better than 5  $\mu\text{in.}$ , RA. The compressive residual stress distributions produced by 8A SP, gravity peening, and three cycles of LSP are compared to a single pass LPB processing of IN718 in Figure 7. Note the low cold working produced by both LSP and LPB compared to SP. LPB can produce higher magnitude and deeper compression than LSP. Using large tooling, LPB has produced a depth of compression to 0.5 in. (12 mm) on a conventional machine tool.<sup>24</sup>

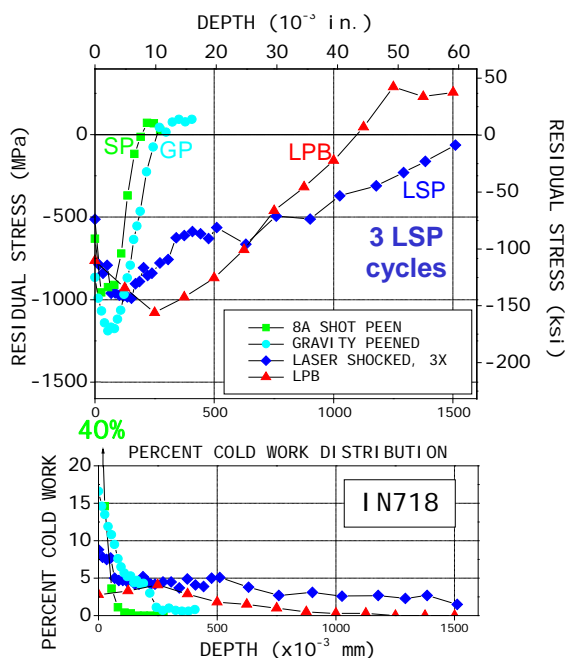


**FIGURE 7** – Comparison of LSP, LPB, SP and gravity peening depth of compression

### X-RAY DIFFRACTION, RESIDUAL STRESS AND COLD WORK DETERMINATION

X-ray diffraction (XRD) residual stress measurements are made employing a  $\sin^2\psi$  technique and the diffraction of the radiation appropriate for the alloy. It was first verified that the lattice spacing was a linear function of  $\sin^2\psi$  as required for the plane stress linear elastic residual stress model.<sup>29,30,31</sup> Subsurface residual stress distributions are determined by making measurements as a function of depth by incremental electropolishing to the final depth. Subsurface residual stress measurements are corrected for both the penetration of the radiation into the subsurface stress gradient<sup>29</sup> and for stress relaxation caused by layer removal.<sup>32</sup> The value of the x-ray elastic constants required to calculate the macroscopic residual stress from the crystal lattice strain are determined in accordance with ASTM E1426-91.<sup>33</sup> Systematic errors are monitored per ASTM specification E915.

The  $K\alpha_1$  peak breadth is calculated from the Pearson VII function fit used for peak location during macroscopic stress measurement.<sup>34</sup> The percent cold work is calculated using an empirical relationship established between the material cold working (true plastic strain) and the  $K\alpha_1$  line broadening.<sup>35</sup> The percent cold work is a scalar quantity, taken to be the true plastic strain necessary to produce the diffraction peak width measured based on the empirical relationship.

### HIGH CYCLE FATIGUE TESTS

HCF tests on laboratory specimens, special component feature specimens and actual components were performed in the untreated and LPB treated conditions on a Sonntag SF-1U machine at room temperature at a frequency of 30 Hz. Thick section fatigue specimens were tested to characterize the

baseline material behavior, the effect of fretting damage, and the general benefits of LPB. These test methods have been adequately described previously.<sup>14,36</sup> Only results from these tests will be discussed in this paper. Because microcracking found in turbine engine dovetail joints is difficult, if not impossible to duplicate in the laboratory, microcracking an order of magnitude deeper than that produced by fretting was simulated in laboratory tests of components using EDM (electrical discharge machining) V-shaped notches that were nominally 0.1 in. (2.5 mm) long, 0.005 in. (0.125 mm) wide, and either 0.020 in. (0.5 mm) or 0.030 in. (0.75 mm) deep. Because fretting-induced microcracks are less than 0.005 in. (0.13 mm) deep, the EDM notches were considered to be substantially more aggressive than actual fretting damage. Mitigation of naturally induced fretting fatigue cracks in test samples has been reported previously.<sup>14,17,18</sup>

## RESULTS AND DISCUSSION

### FATIGUE DESIGN

Residual stress distribution design was based upon a value of  $k_f$  determined empirically from HCF tests conducted on laboratory coupons of Ti-6Al-4V. Figure 8(a) shows the HCF S-N data for the baseline (untreated) condition tested at R ( $S_{min}/S_{max}$ )=0.1 with and without active fretting produced during testing (as apposed to prior fretting damage). It is evident that active fretting leads to substantial fatigue debit. At a fatigue life of  $10^7$  cycles, the effective fatigue stress concentration factor,  $k_f$ , is nominally 2.6. When this damage condition is applied to the FDD, the baseline nominal fatigue strength and the fatigue strength under active fretting condition can be plotted as shown in Figure 8(b). The  $RS_{min}$  of nominally -40 ksi (-276 MPa) is predicted to restore the fatigue performance, and compression in excess of that is predicted to show some benefit over the nominal fatigue strength of the baseline condition, even with the fretting damage. In this particular specimen group LPB generated a RS distribution as shown in Figure 9(a). The corresponding fatigue performance of LPB treated specimens without and with active fretting damage, shown in Figure 9(b), indicates that the LPB treated specimens indeed showed an improved performance over the baseline condition. These initial coupon tests demonstrated that full mitigation of fretting damage fatigue can be achieved in Ti-6-4 with LPB treatment. In this initial investigation, the effects of compensatory tension leading to subsurface initiation, and the ensuing fatigue cracking from that region were also predicted by the FDD.

### LPB TREATED BLADE DOVETAIL AND DISK POST CONTACT REGIONS

Compressor blade dovetail contact regions were LPB treated using the tool shown in Figure 5(a). As indicated earlier, the single point tool was controlled by a previously designed CNC tool path and by applying appropriate pressures synchronized to the tool position. A photograph of the LPB treated blade is shown in Figure 10(a). The LPB residual stress distribution measured by x-ray diffraction is shown in Figure 10(b). This graph shows the residual stress as a function

distance with respect to the edge of bedding on the surface of the blade dovetail as a function of depth at 0.005, 0.010, 0.020, 0.040 and 0.060 in. (0.125, 0.25, 0.5, 1 and 1.5 mm) respectively. It is evident from this figure that the compression extended to a depth in excess of 0.050 in. (1.25 mm) even though the radius at the platform of the dovetail was not processed, due to the geometry of this region, Subsurface compression was evident due to the compression developed in the contact surface.

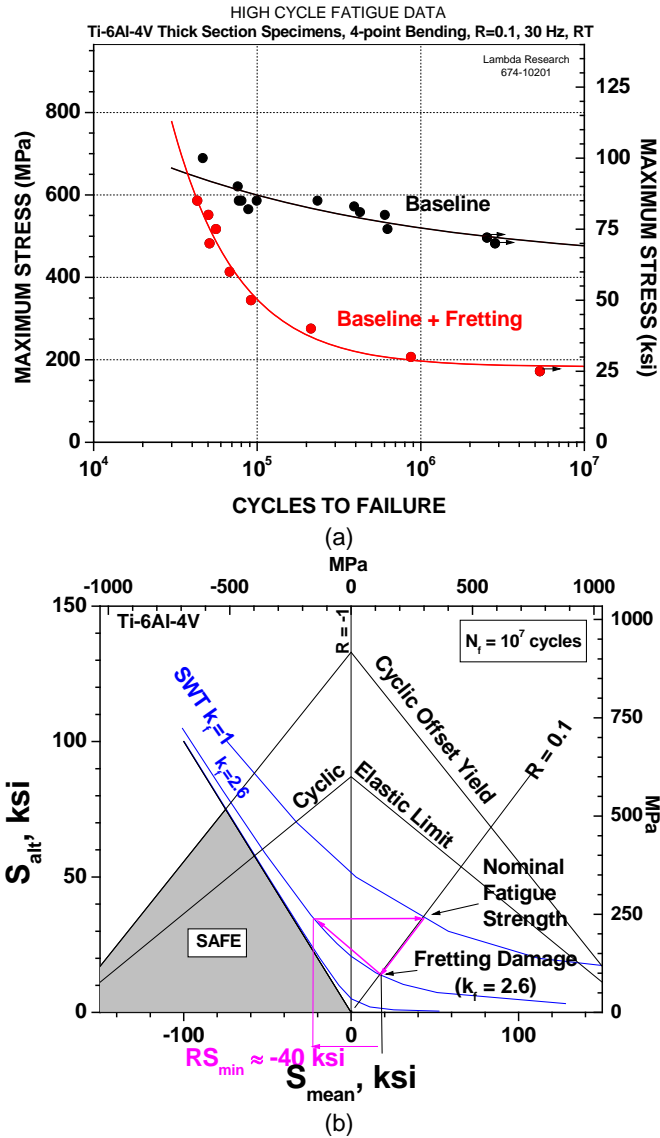


**FIGURE 8 - (a)** S-N data showing the fretting fatigue results for Ti-6Al-4V test specimens in the baseline (untreated) condition. **(b)** FDD with the SWT line for the effective  $k_f \approx 2.6$

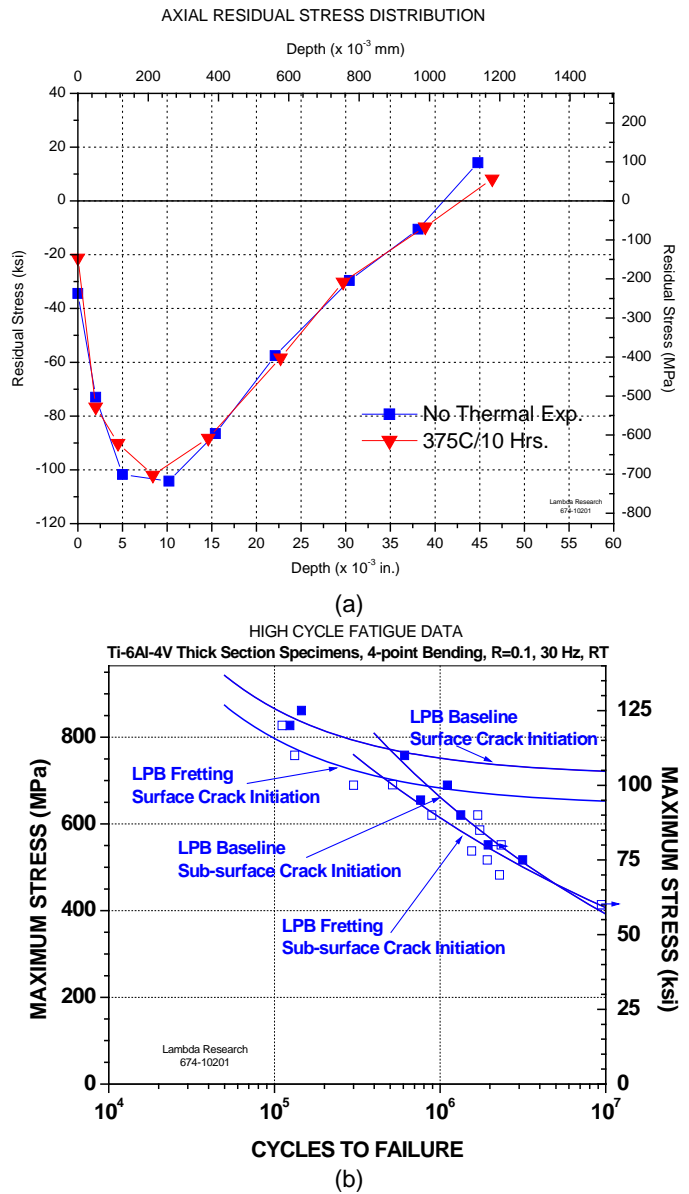


**FIGURE 9 - (a)** Residual stress profile as a function of depth in LPB treated specimen. **(b)** S-N data showing the fretting fatigue results for Ti-6Al-4V test specimens in the LPB treated conditions.

In order to understand the effect of compression on the location and magnitude of compensatory tension, a finite element analysis (FEA), shown in Figure 11, was constructed with the LPB-induced compression. It is evident in this figure that the compensatory tension is located near the thick bottom of the dovetail section, below the layer of high compression, and away from the critical high stress fretting damaged regions, where it does not contribute to fatigue failure under service loading. The material on the dovetail surface beyond the LPB processed zone, is seen to be forced into compression by the adjacent highly compressive LPB processed zone.



(a)

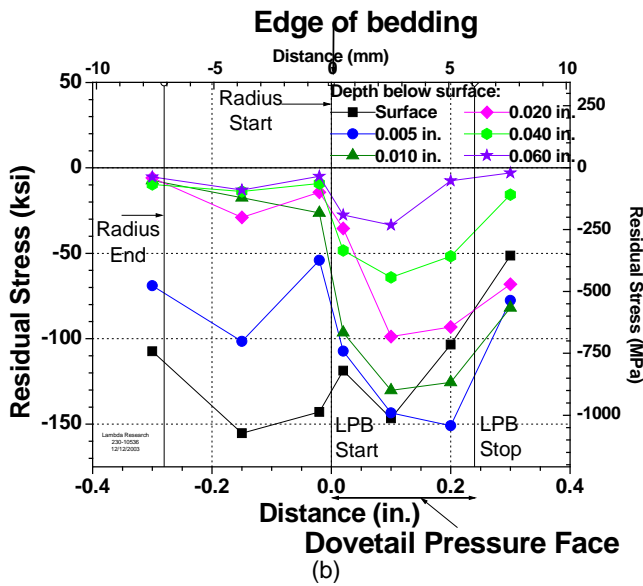


FIGURE 10 - (a) LPB treated compressor blade dovetail contact region, (b) Residual stress distribution on the dovetail section of the LPB treated blade.

Based on the residual stresses achieved in the dovetail, the fretting fatigue damage should be completely mitigated by the LPB process. HCF tests were conducted on untreated and LPB treated blade dovetails. As indicated earlier, since fretting damage on actual components is very difficult to simulate in laboratory test conditions, an extreme fretting induced microcrack damage was simulated with a 0.020 in. (0.5 mm) or a 0.030 in. (0.75 mm) deep EDM notch. Because the typical fretting-induced microcrack is shallower than 0.003 in. (0.075 mm), the 0.020 in. (0.5 mm) deep EDM notch is a more aggressive damage condition compared to fretting damage. Figure 12 shows the S-N data for these test conditions. The baseline (untreated) blades with 0.020 in. (0.5 mm) notch failed with a run-out condition at  $10^7$  cycles of about 30 ksi (207 MPa). The LPB treated blades with 0.020 in. (0.5 mm) notch did not fail from the notch, even when tested at stresses of about 90 and 100 ksi (620 to 690 MPa), thus showing better than a factor of 3 improvement over the untreated blades. The

LPB treated blades with a 0.030 in. (0.75 mm) notch showed almost a factor of 2 improvement in fatigue strength (at greater than  $10^6$  cycles) over the untreated blades with 0.020 in. (0.5 mm) well above the customary  $k_t = 3$  design criteria.

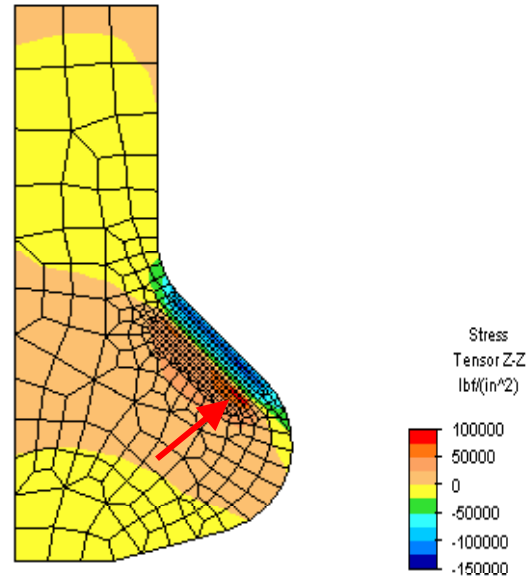


FIGURE 11 - FEA simulation of the residual stresses from Figure 10(b) identifies the location (red arrow) and magnitude of the compensatory tensile residual stresses in the blade.

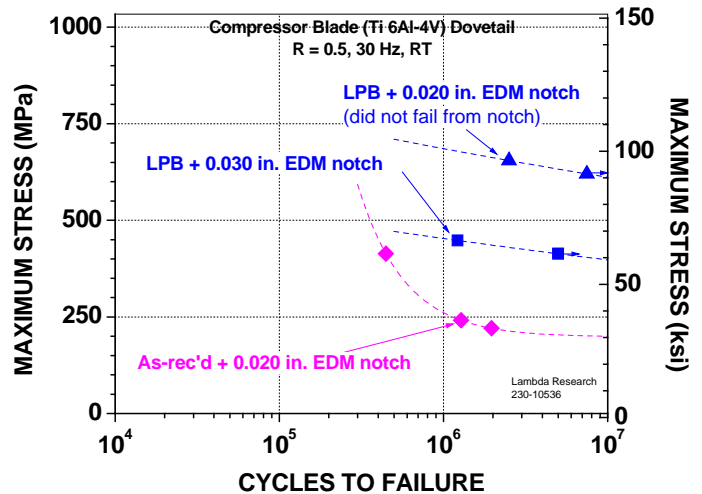


FIGURE 12 - S-N data for the compressor blades

Based upon the compressive residual stress distribution and fatigue performance achieved in the compressor blade dovetail, a comparable compressive distribution was designed for the compressor disk post contact region. An LPB tool designed to simultaneously process the two sides of the disk post is shown in Figure 5(b). A photo of the LPB treated disk post after removal from the compressor disk is shown in Figure 13. The residual stress distribution for the disk post contact region after LPB treatment is shown in Figure 14. As expected,

the results in this figure are comparable to the residual stress distribution shown for the compressor blade dovetail contact region in Figure 10(b). Similar to the blade dovetail contact region EOB, the disk post contact region EOB shows a depth of compression better than 0.040 in. (1 mm). This verifies the fact that the LPB process parameters chosen for the disk post region are effective in producing the desirable residual stress distribution capable of mitigating fretting damage on the disk post contact surface.



**FIGURE 13** – Photo of the LPB treated disk post. This post was removed from the compressor disk after LPB treatment.

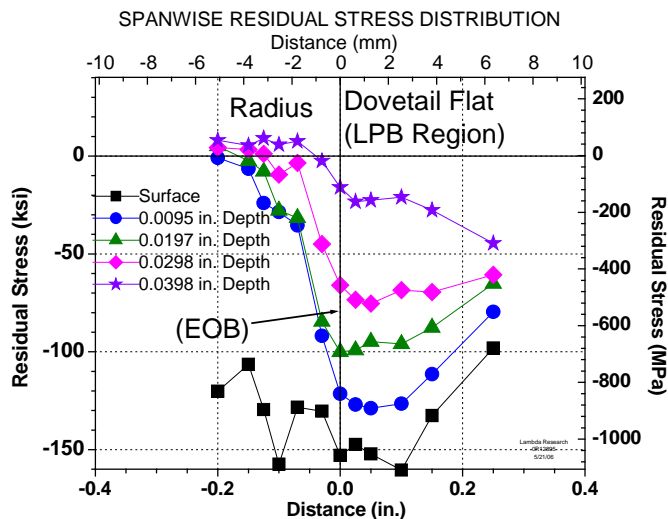


**FIGURE 14** - Residual stress distribution on the compressor disk post dovetail contact region after LPB treatment. These results are comparable to Figure 10(b) for the blade dovetail contact surface.

## SUMMARY AND CONCLUSIONS

LPB tooling technology has been developed to introduce deep high magnitude compression on the pressure faces of fan and compressor blade dovetails and mating disk slots. A FDD method has been demonstrated to determine the magnitude of compression needed to restore and even improve the fatigue

strength of fretting damaged titanium alloy compressor components. Fretting induced micro-cracks that form at the EOB on the pressure face of both the blade dovetail and the disk slots in Ti-6Al-4V compressor components were simulated with 0.020 and 0.030 in. (0.5 and 0.75 mm) deep EDM notches designed to produce a more aggressive damage condition than the shallow (less than 0.005 in. (0.125 mm) deep) fretting-induced microcracks. LPB processing introduced the designed compressive layer that not only mitigated the simulated damage, but also provided fatigue performance superior to the baseline condition, as predicted by the FDD. The introduction of deep stable compression using conventional CNC machine tools during manufacture or overhaul to restore and improve the fatigue performance of fretting dovetail joints in titanium alloy compressor components has been demonstrated. The compressive residual stress field design method employing the FDD approach was shown to be fully applicable to completely mitigate fretting damage in Ti-6Al-4V. The depth and magnitude of compression and the fatigue and damage tolerance achieved are reproducible with different LPB tools to process coupons for fatigue testing, the blade dovetail contact face, and the mating disk slots. It was found that micro-cracks as deep as 0.030 in., large enough to be readily detected by current NDI technology, can be fully arrested by LPB. The depth of compression achieved could allow NDI screening followed by LPB processing of critical components to reliably restore fatigue performance, minimize inspection requirements, and extend component life.

## REFERENCES

- 1 C. Ruiz, P.H. B. Boddington and K.C. Chen, (1984) "An Investigation of Fatigue and Fretting in a Dovetail Joint," *Experimental Mechanics*, Vol. 24, No.3, September, pp 208-217.
- 2 B.A. Cowles, (1989) "High Cycle Fatigue In Aircraft Gas Turbines—An Industry Perspective," *International Journal of Fracture*, Vol. 80, No.2-3, April, pp 147-163.
- 3 T. Nicholas, (1999) "Critical Issues in High Cycle Fatigue," *International Journal of Fatigue*, Vol. 21, Supplement 1, September, pp 221-231.
- 4 D.A. Hills and D.A. Nowell, (1994) *Mechanics of Fretting Fatigue*, Dordrecht, Kluwer Academic
- 5 Y. Kondo & M. Bodai, (2001) "The Fretting Fatigue Limit Based On Local Stress At The Contact Edge," *Fatigue & Fracture of Engineering Materials & Structures*, Vol. 24, Issue 12, December, pg 791.
- 6 M.P. Solwinski, T.N. Farris, (1996) "Mechanics of Fretting Fatigue Crack Initiation," *Wear*, Vol. 198, pp 193-207.
- 7 S. A. Namjoshi, S. Mall, V. K. Jain and O. Jin, (2002) "Fretting Fatigue Crack Initiation Mechanism In Ti-6Al-4V," *Fatigue & Fracture of Engineering Materials & Structures*, Vol. 25, Issue 10, October, pg. 955
- 8 K. Sato, H. Fujii, S. Kodama, (1986) "Crack Propagation Behavior in Fretting Fatigue," *Wear*, Vol. 107, pp 245-162.

- 9 D.L. Anton, R. Guillemette, J. Reynolds, M. Lutian, (1997) "Fretting Fatigue Damage Analysis in Ti-6Al-4V," Surface Performance of Titanium, Ed. J.K. Gregory, H.J. Rack, D.Eylon, The Minerals, Metals and Materials Society.
- 10 S. Suresh, (1998) Fatigue of Materials, 2nd edition, Cambridge University Press, pg. 462.
- 11 T.A. Venkatesh, etal, (2001) "An Experimental Investigation of Fretting Fatigue in Ti-6Al-4V – the Role of Contact Conditions and Microstructure," *Metallurgical and Materials Transactions A*, Vol. 32A, May, pp 1131-1146.
- 12 R. K. Betts, (2006) "Copper-Nickel-Indium, a Classic Basis for Coating Development," 17th AeroMat Conference and Exposition, May 15-18, Seattle, WA
- 13 S. A. Namjoshi, S. Mall, V. K. Jain and O. Jin, (2002) "Effects of Shot-Peening on Fretting-Fatigue Behavior of Ti-6Al-4V," *Journal of Engineering Materials and Technology*, April, Vol. 124, Issue 2, pp. 222-228.
- 14 M. Shepard, P. Prevéy, N. Jayaraman, (2003) "Effect of Surface Treatments on Fretting Fatigue Performance of Ti-6Al-4V," *Proceedings of the HCF Conference*, Monterey, CA, April 14-16.
- 15 H. Soyama, D.O. Macodiyo and S. Mall, (2004) "Compressive Residual Stress into Titanium Alloy Using Cavitation Shotless Peening Method," *Tribology Letters*, Vol. 17, Number 3, October, pp. 501-504.
- 16 D. Sokol, A. Clauer, D. Lahrman, D. See, L. Bernadel, (2006) "Laser Peening for Improved Fretting Fatigue Life," 17th AeroMat Conference and Exposition, May 15-18, Seattle, WA.
- 17 N.R. Lovrich, X.Huang, R. Neu, (2006) "Effect of Low Plasticity Burnishing on Fretting Fatigue of Ti-6Al-4V," *Fatigue 2006, Conference Proceedings*, Atlanta, May.
- 18 P.J. Golden, (2006) "Development of a Dovetail Fretting Fatigue Fixture for Turbine Engine Materials," *Propulsion – Safety and Affordable Readiness (P-SAR) 2006 Conference Proceedings*, 28-30 March, Jacksonville, FL.
- 19 S. Chakravarty, etal,(1995) "Research Summary: The Effect of Surface Modification on Fretting Fatigue in Ti Alloy Turbine Components," *Journal of Metals*, Vol. 47, Number 4, April, pp 31-35.
- 20 D. Liu, etal, (1999) "Improvement of Fretting Fatigue and Fretting Wear of Ti6Al4V by Duplex Surface Modification," *Surface and Coatings Technology*, Vols. 116-119, pp 234-238.
- 21 AFGROW Fracture Mechanics Program, ver. 4.0009e.12, <http://www.afgrow.wpafb.af.mil>
- 22 P. Prevéy, N. Jayaraman, R. Ravindranath, (2005) "Design Credit for Compressive Residual Stresses in Turbine Engine Components," *Proceedings of the HCF Conference*, New Orleans, LA, March 8.
- 23 K.N. Smith, P. Watson, T.H. Topper, (1970), "A Stress-Strain function for the Fatigue of Metals," *Journal of Materials*, Vol. 5, No. 4, pp 767-778.
- 24 N. Jayaraman, P.I. (2005) "Design Tools For Fatigue Life Prediction In Surface Treated Aerospace Components", NAVY SBIR Topic: N05-026 Phase I Final Report, September 30.
- 25 U.S. Patent 5,826,453 (Oct. 1998), other US and Foreign patents pending.
- 26 P. Prevéy, (2000), "The Effect of Cold Work on the Thermal Stability of Residual Compression in Surface Enhanced IN718," Proc. 20th ASMI Conference.
- 27 NAVAIR Phase I SBIR Final Report (2001) Contract N68335-01-C-0274 NAVAIR, "Affordable Compressor Blade Fatigue Life Extension Technology," Nov. 29.
- 28 Air Force Phase II SBIR (2003), Contract F33615-03-C-5207, "Component Surface Treatments for Engine Fatigue Enhancement"
- 29 A. Ahmad, C. Ruud, P. Prevéy, ed., (2003), Residual Stress Measurement by X-Ray Diffraction, HS-784, SAE, Warrendale, PA.
- 30 I.C. Noyan and J.B. Cohen, (1987) Residual Stress Measurement by Diffraction and Interpretation, Springer Verlag, New York, NY.
- 31 B.D. Cullity (1978) Elements of X-ray Diffraction, 2nd ed., Addison-Wesley, Reading, MA, pp. 447-476.
- 32 M.G. Moore and W.P. Evans, (1958) "Mathematical Correction for Stress in Removed Layers in X-Ray Diffraction Residual Stress Analysis," *SAE Transactions*, Vol. 66, pp. 340-345
- 33 P. Prevéy, (1977), "A Method of Determining Elastic Properties of Alloys in Selected Crystallographic Directions for X-Ray Diffraction Residual Stress Measurement," Adv. In X-Ray Analysis, 20, Plenum Press, New York, NY, pp 345-354.
- 34 P. Prevéy, (1986) "The Use of Pearson VII Functions in X-Ray Diffraction Residual Stress Measurement," Adv. in X-Ray Analysis, 29, Plenum Press, New York, NY, pp 103-112.
- 35 P. Prevéy, (1987), "The Measurement of Residual Stress and Cold Work Distributions in Nickel Base Alloys," Residual Stress in Design, Process and Material Selection, ASM, Metals Park, OH.
- 36 P. Prevéy, N. Jayaraman, R. Ravindranath, (2005) "Use of Residual Compression in Design to Improve Damage Tolerance in Ti-6Al-4V Aero Engine Blade Dovetails," *Proceedings of the 10th HCF Conference*, New Orleans, LA, March 8-11.